Lawrence Berkeley National Laboratory
Recent Work

Title

STRUCTURE AND PROPERTIES OF DYNAMICALLY STRAIN AGED STEELS

Permalink

https://escholarship.org/uc/item/7fv8q7rm

Authors

Page, E.W.
Mangonon, P.
Thomas, G.
et al.

Publication Date

1968-09-01

ey. 2

University of California

Ernest O. Lawrence Radiation Laboratory

STRUCTURE AND PROPERTIES OF DYNAMICALLY STRAIN AGED STEELS

E. W. Page, P. Mangonon, Jr., G. Thomas, and V. F. Zackay

September 1968

Berkeley, California

UCRL - 18386 ey. 2

DISCLAIMER

UNIVERSITY OF CALIFORNIA

Lawrence Radiation Laboratory
Berkeley, California

AEC Contract No. W-7405-Eng-48

STRUCTURE AND PROPERTIES OF DYNAMICALLY STRAIN AGED STEELS

E. W. Page, P. Mangonon, Jr., G. Thomas and V. F. Zackay

September 1968

STRUCTURE AND PROPERTIES OF DYNAMICALLY STRAIN AGED STEELS

E. W. Page, P. Mangonon, Jr., G. Thomas, and V. F. Zackay

Inorganic Materials Research Division, Lawrence Radiation Laboratory,
Department of Mineral Technology, College of Engineering,
University of California, Berkeley, California

ABSTRACT

The introduction of small amounts of plastic deformation (2-5%) during
the conventional heat treatment of tempered martensitic steels either between
tempering stages (static strain aging) or during tempering (dynamic strain
aging) can confer significant increases in strength without serious losses
of ductility.

This investigation deals with the structure and properties obtained by
dynamic strain aging of Fe/Cr/C and Fe/Mo/C steels. The structures were
investigated using transmission electron microscopy and diffraction of foils
and extraction replicas. Microprobe techniques were also employed.

After quenching the structure consists of auto-tempered Widmanstatten
cementite plates in a dislocated matrix. After dynamic strain aging, there
is evidence for an increase in dislocation density and also for plastic
deformation of the carbide plates.

The results lead to the conclusion that dynamic strain aging provides
an increase in strength which is limited by the ultimate tensile strength
of the steel, i.e. by work hardening. An increase in strength beyond this
limit is only achieved in the Fe/Mo/C steel when dynamic strain aging pro-
duces secondary hardening through precipitation of an alloy carbide. Al-
though chromium does not produce secondary hardening, the Fe/Cr/C steel is
superior to the Fe/Mo/C steel regarding both strength and ductility.

Overaging of the Fe/Cr/C steel is due to recovery, recrystallization
and growth of cementite particles. Recovery and recrystallization is not
observed, at the same temperatures, in the Fe/Mo/C steel.

I. INTRODUCTION

Efforts to improve both the strength and ductility of steels have traditionally centered on modifications in composition or variations in the heat treatment. However, utilizing conventional strengthening techniques, an inverse relationship between strength and ductility is usually observed (for review see e.g. ref. 1).

Thermomechanical processes, such as ausforming and dynamic strain aging (for convenience this process will be referred to as DSA in this paper), where plastic deformation at elevated temperatures is introduced into the heat-treatment cycle, have been developed which increase the strength without significant losses in ductility or toughness (2-10).

Much work has been done on the mechanical properties of dynamically strain aged low alloy martensitic steels, but attempts to relate the microstructures with the properties of these steels were inconclusive (8).

This paper describes a more detailed investigation in an attempt to clarify the important strengthening mechanism (s) occuring in the dynamic strain aging process. The compositions of the steels used for this investigation are shown in Table I.

Table I.   Chemical Composition, wt.%.

Steel	% C	% Alloying Element	Balance	Ms[a] (°C)
Fe-Mo-C	.187	3.38 Mo	Fe	400
Fe-Cr-C	.186	3.58 Cr	Fe	440

(a) Calculated, based on K. W. Andrews, J. Iron, Steel Inst. 203, 721

   (1965).

II. EXPERIMENTAL

A. Preparation

The materials used in this study were vacuum-induction-melted from high purity iron, chromium and molybdenum and cast into 20 lb ingots. The as-cast ingots were homogenized for 100 hrs at a temperature of 1100°C in a pure helium atmosphere in order to minimize decarburization. The chemical analysis obtained on sections of the ingots are shown in Table I.

The ingots were forged and cut into sections 6" by 3" by 1/8", austenitized at a temperature 1200°C for 30 minutes in a pure helim atmosphere, quenched in water, and finally, stored at liquid nitrogen temperatures.

B. Thermomechanical Treatments

After water quenching, both steels were tempered at 600°C, 500°C, 375°C, 250°C, 125°C, and room temperature, respectively. Dynamic strain aging by rolling to approximately 5% strain was also carried out at these temperatures. In order to minimize heat losses during rolling, the rolls were preheated to 200°C. It was found that holding for up to 30 minutes at processing temperature, either before or after 5% deformation, had no effect on the resulting mechanical properties.

C. Mechanical Tests

The steels were tested in tension using a cross-head speed of 0.04 in/min after all treatments. Specimens 6" x 7/8" x 1/8" with a 2-in gauge length were used for this purpose.

D. Microscopy

Specimens were examined by light optical metallography and then sections suitable for transmission electron microscopy were prepared from the heat treated steels, by chemical thinning followed by electropolishing in the usual way. In addition, carbon extraction replicas were prepared after all the processing steps. Foils and replicas were examined in a Siemens Elmiskop 1 microscope operated at 100kV, utilizing bright- and dark-field imaging techniques together with selected area diffraction. A thin layer of gold was vacuum evaporated on portions of replicas for standardizing the diffraction measurements. In addition, a MAC model 400 microprobe analyser was used for chemical analysis of the extraction replicas.

III. RESULTS

A. Mechanical Properties

The effect of the DSA treatment upon the tensile properties is shown in Figs. 1-3. A general increase in yield strength of about 15% was obtained after DSA of both steels (Fig. 1,) which is similar to the results obtained by Wilson and Russell (11). Upon dynamic strain aging at 375°C, the Fe/Mo/C alloy showed a secondary hardening peak. Although there is a maximum increase in yield strength of 46%, there is only about a 12% increase over the highest yield obtained by tempering alone (Fig. 1). Both alloys overage after treatment above about 375°C. As is well known (12), at these alloy contents, chromium is a more effective strengthener than molybdenum, e.g. both in the tempered and DSA treated conditions, even the yield of the secondary hardened Fe/Mo/C steel is no greater than that of the Fe/Cr/C steel treated at the same temperature. (Fig. 1).

Similar trends are observed in the UTS, although the strength increment is not as great as that in yield (Fig. 2). Figure 3a,b indicates there is only a small sacrifice in uniaxial tensile ductility following the rolling deformation used in the DSA. It is significant to note that the ductility of the Fe/Cr/C steel over the whole temperature range is superior to that of the Fe/Mo/C steel both in the tempered and DSA conditions. Experiments done to age the steels for 30 minutes prior to DSA at the same temperature showed no significant differences when compared to the normal DSA treatment.

The results of Figs. 1-2 show that a plastic strain of 5% work hardens the steel to its capacity, i.e., its ultimate strength. This is illustrated in Fig. 1 by the fact that the yield strengths of the DSA steels are the same as the ultimate strengths of the quenched and tempered steels.

Indeed, the only significant gain in strength that can be achieved by DSA occurs when the latter causes secondary hardening as shown in Fig. 2. Tempering to 375°C causes some softening, whereas, 5% strain at 375°C produces hardening. If DSA is not employed in the Fe/Mo/C steels, tempering at 600°C is required for secondary hardening to occur (see for example, Honeycombe et. al., (13). It should be noted, however, that although secondary hardening is produced in the Fe/Mo/C steel, the strength level achieved does not exceed that which is obtained in the non-secondary hardening Fe/Cr/C steel (Figs. 1,2).

B. Microprobe

Microprobe analysis was carried out using extraction replicas from the DSA specimens. Standards of pure Fe, Cr and Mo were used to measure the sensitivity of the radiation to the pure samples. Background counts of Fe, Cr, and Mo were measured on pure C and Cu standards, since the replicas were made with carbon and placed on Cu grids.

It was found that only the samples after DSA at 500°C gave counts above the base level. This result enables us to identify the presence of chromium, and molybdenum respectively only in precipitates extracted from samples given the 500°C treatment.

C. Electron Microscopy

1. As-Quenched Steels

The microstructure of both as-quenched steels consists of a Widmanstatten morphology of auto-tempered precipitates in a dislocated matrix. This structure is expected in steels of relatively high Ms temperatures (Table I). An example for the Fe/Cr/C steel is shown in Fig. 4, which is

identical to the structure of the Fe/Mo/C steel. The precipitates were

identified to be Fe_3C as a result of examination of many differently oriented

foils as well as by extraction replicas. Trace analysis of the various

foils showed that the cementite particles precipitate on {110} and are

aligned along the <111> directions. The orientation relationship between

cementite and α-matrix is found to correspond to the Pitsch - Schrader

relation (14). The precipitation is a result of auto-tempering during the

quench and this microstructure is typical for steels with relatively high

M_s temperatures (calculated to be about 400°C for the Fe/Mo/C steel and

440°C for the Fe/Cr/C steel). Occasionally, some twinning was also observed

as can be seen in the region marked C in Fig. 4a. These observations are

similar to those observed by other researchers (15-20).

Contrast effects can be seen around the cementite particles in the

bright field image, but not in the dark field image using only cementite

reflections (e.g. Fig. 4a,b). These contrast effects probably arise from

dislocation tangles and loops. The precipitates themselves are not deformed.

2. Non-Deformed Steels -- Effect of Tempering

No observable change in the number or size of the auto-tempered preci-

pitates in either steel occurred until the tempering temperature was 375°C

or higher. Figures 5a and b illustrate this effect in the Fe/Mo/C steel.

These results are in agreement with those of Baker and Kelly (15). Tempering

at 500°C produces growth and spheroidization of the carbides. At 600°C, in

the Fe/Cr/C steel recovery of dislocations and partial recrystallization

also occurs particularly after DSA, as shown in Fig. 6, but not in the

Fe/Mo/C steel as shown in Fig. 7.   Associated with these changes is the

drop in yield and tensile strengths for both steels, as shown in Figs. 1

and 2.

3. Dynamic Strain Aging

The following microstructural changes caused by DSA were observed:
(1) an increase in dislocation density around the pre-existing auto-tempered
precipitates; (2) distortion of the prior existing auto-tempered precipitates
themselves; (3) precipitation of very small particles on dislocations in
both steels after DSA at 375°C and (4) in the Fe/Mo/C alloy precipitation
of a molybdenum carbide was tentatively identified after treatment at 500°C.
Micrographs illustrating these effects are shown in Figs. 6, 8, 9, which
should be compared to Fig. 4.

The observations concerning the increase in dislocation density and
the distortion of the existing precipitates are based on a detailed com-
parison of the bright- and dark-field images of the steels in the DSA and
quenched and tempered conditions. For example, Fig. 8 a and b from the
Fe/Cr/C steel after DSA at 125°C shows that the cementite particles observed
in the dark-field image of (b) are more distorted and exhibit more internal
strain than those precipitates in the quenched and tempered steels, e.g.
Fig. 4b. It also appears that the matrix around the particles is more dis-
torted after DSA treatment (compare Figs. 8, 4 and 5). These observations
indicate that the precipitates are effective barriers to plastic deformation.

It is estimated (7-18) that the dislocation density in untempered dis-
located martensites is about 10^{12}/cm^2. An increase in density by a factor
of two can account for the increase in flow stress produced by 5% plastic
deformation. Whilst such an increase in dislocation density cannot be
measured by electron microscopy, our observations (e.g. Fig. 8) indicate
dislocation motion and subsequent dislocation multiplication at the particles.
Thus, we conclude that the main strengthening effect of DSA is work hardening
through an increase in dislocation density.

After DSA, there is evidence for precipitation on dislocations particularly in steels treated at 375°C. In order to see these precipitates, the dislocations have to be tilted out of contrast as shown in Fig. 9. It was not possible to identify uniquely such small precipitates. Only Fe_3C reflections were observed, in addition to matrix bcc reflections, in the diffraction patterns. The fact that these precipitates seem to lie along the dislocations with no dislocation tangles around them, (as occurs with the auto-tempered Fe_3C precipitates), indicates that their nucleation is a result of heterogeneous precipitation during DSA.

These small precipitates could form as a result of dissolution and re-precipitation of the Fe_3C on dislocations after the plastic deformation. Since these precipitates are only clearly observed after DSA at 375°C, and since the increases in yield strength observed in Fig. 1 are independent of processing temperature, it is concluded that these precipitates do not significantly contribute to the strengthening process.

Figures 1 and 2 show that after DSA at 375°C, the Fe/Mo/C steel exhibits a secondary hardening peak. This phenomenon is most likely to be due to precipitation of an alloy carbide such as Mo_2C, as has been proposed by Honeycombe et al. (13,21) to account for secondary hardening after normal tempering in the range 500°C - 600°C.

Many attempts were made to prove this but only limited results were obtained. For example, different foils and extraction replicas were investigated by selected area diffraction and dark field techniques. Table II shows a summary of the d-values obtained. Only in a few instances do the results indicate the possibility of the presence of Mo_2C (or Fe_2Mo C), and then only after the 500°C and 600°C treatments. This evidence alone is

obviously unsatisfactory, but it is always difficult in electron diffraction

to make unambiguous distinctions because of the similarities in spacings

between iron and molybdenum carbides, and because of the large multiplicity

of reflections, e.g. due to double diffraction. Thus it is impossible to

distinguish separately Fe_3C and Mo_2C by dark-field techniques. However, we

do find morphological differences in precipitation before and after second-

ary hardening, particularly at the highest temperatures. Figure 7 a,b shows

a foil obtained after 30 minutes tempering at 600°C. The dark-field image

Fig. 7b of the streak in Fig. 7 near the $(1\bar{1}0)$ spot reverses contrast at

the thin plates, and since an Fe_3C reflection is also included, the sphero-

dized cementite also reverses contrast as shown at B. The streak lies nor-

mal to these plates as expected. The position of this streak corresponds to

a predicted Mo_2C reflection, and agrees with the conclusions of Honeycombe

et al. (13,21). Furthermore, there is a marked difference in morphology

between the thin plates in Fig. 7 and the usual Widmänstatten pattern of

Fe_3C, e.g. compare Figs. 5, 7, and 8, which are all in [311]. Finally,

electron microprobe analyses of carbide extractions after the 500°C and 600°C

treatments definitely showed the presence of molybdenum. Thus, we tentatively

conclude that the secondary hardening peak after DSA is due to precipitation

of an alloy carbide, but it is not possible to uniquely determine which

carbide is present.

Similar attempts to find evidence for carbides other than Fe_3C in the

Fe/Cr/C steel were totally unsuccessful. Although electron microprobe

analysis of extracted carbides from a steel after DSA at 500°C and 600°C

showed the presence of chromium, there was no detectable change in carbide

morphology other than coarsening (Fig. 6). This suggests that chromium

simply replaces iron in the cementite {it is thought that Cr_7C_3 forms in-situ

from Fe_3C (22,23) althought this idea has been disputed (24)}, and this is

consistent with the fact that the Fe/Cr/C steel does not secondary harden.

Treatments above 375°C produce softening, and in the Fe/Cr/C steel, consid-

erable recovery and recrystallization as well as spherodization of cementite,

e.g. Fig. 6. Except for some spherodization, these effects are not observed

in the Fe/Mo/C steel (Fig. 7).

Table II - Analysis of Diffraction Patterns from Fe/Mo/C steel
          after DSA Treatments at 500°C, 600°C.

Fe_3C[a]	Observed "d" values	Mo_2C[a]
2.81		
2.75	2.60	2.60
2.55	2.56	
2.38	2.38	2.38
2.37	2.37	2.37
2.26	2.28	2.28
2.14	2.17	
2.10	2.10	
2.06	2.08	
1.75	1.75	1.75
1.35		1.35
1.33		1.30
1.27	1.29	1.27
1.25		1.26
1.20		
1.19	1.19	
	1.16	1.18
	1.14	1.14
1.07	1.09	1.07
	0.98	0.98

(a) Values from ASTM index file.

IV. DISCUSSION AND CONCLUSIONS

The principal conclusion arising from this investigation is that

dynamic strain aging provided an increase in strength which was limited

only by the ultimate tensile strength of the steel, i.e. by work hardening.

An increase in strength beyond this limit was only achieved in the Fe/Mo/C

steel when the DSA treatment produced secondary hardening through precipi-

tation of any alloy carbide tentatively concluded to be Mo_2C. Under all

conditions of treatment, however, chromium, although not producing secondary

hardening, is more effective than molybdenum as a strengthening alloying

element (Figs. 1-3).

The structural features and associated observed mechanical properties

of DSA steels can be summarized as follows:

(1) Since the Ms temperatures of these low alloy steels is high,

during quenching to martensite, cementite forms and auto-tempers to a well

defined Widmanstatten pattern. The substructure consists of these precipi-

tates in a dislocated matrix with occasional evidence for micro-twinning.

No change in morphology was observed up to 375°C.

(2) The plastic deformation involved in the DSA processing results

in dislocation movement through the matrix and around the precipitates formed

from auto-tempering. Various possible dislocation interactions can occur

locally such as cross-slip or loop formation so that the steel work hardens.

Such a mechanism has been proposed by several workers (7,5,10). Eventually,

the local stress due to the high dislocation density near the precipitates

can exceed the yield stress of cementite and the cementite itself will deform.

The resulting microstructure is deformed cementite surrounded by dislocations.

Thus one consequence of DSA (or deformation at room temperature) is to raise

the strength by increasing the dislocation density (work hardening component).

Fine precipitates on dislocations can be observed at 375°C, but there is

no evidence to show that these precipitates contribute significantly to

strengthening.

(3) In addition, however, at higher deformation temperatures, DSA

of the Fe/Mo/C steel causes precipitation of an alloy carbide which gives

an added strengthening component (secondary hardening) to the work hardening

contribution.

These microstructural changes are reflected in the uniaxial tensile

properties of DSA Fe/Cr/C and Fe/Mo/C steels. Thus, the incremental gain

in both yield (about 15%) and tensile strength (about 10%) for both alloys

at deformation temperatures below 375°C is constant within experimental

scatter and is not dependent upon the temperature of deformation. It is

likely that this increase in strength is due only to work hardening, in

agreement with the conclusions of Leslie and Keh (25).

Secondary age hardening in Fe/Mo/C steels is well known for aging

at 500°C and above (13), and is to be expected in steels of the composition

utilized in this study. However, a striking feature of the Fe/Mo/C is the

marked acceleration of the aging reaction as a result of DSA. It is not

unexpected, of course, that plastic deformation at temperature accelerates

the kinetics of aging.

In agreement with the observations of others, no evidence of a

secondary hardening peak was observed in the Fe/Cr/C steels. Honeycombe et

al. (13) have shown that no secondary hardening peak can be detected in

Fe/Cr/C steels containing as much as 9% chromium.

Finally, the overaging process in these two steels appears to be

different. After DSA, above 375°C, the Fe/Cr/C steel softens with recovery,

recrystallization and spherodization and coarsening of cementite particles.
However, in the Fe/Mo/C alloy, after the same treatment, there is considerably
less recovery and no recrystallization, so that the softening must be due
only to coarsening of Fe_3C and the alloy carbide. After normal temp-
ering, the Fe/Cr/C steel recrystallizes at 500°C, but the Fe/Mo/C alloy does
not. Thus, obviously molybdenum raises the recrystallization temperature
more effectively than Cr.

ACKNOWLEDGEMENTS

FIGURE CAPTIONS

Fig. 1   Effect of DSA upon the yield strength of Fe/Cr/C and
          Fe/Mo/C steels as a function of processing temperature.

Fig. 2   Effect of DSA upon the tensile strength of Fe/Cr/C and
          Fe/Mo/C steels as a function of processing temperature.

Fig. 3   The effect of DSA upon the ductility of a) Fe/Cr/C and
          b) Fe/Mo/C steels as a function of processing temperature.

Fig. 4   Thin foil micrographs of Fe/Cr/C steel after quenching;
          [111] orientation; a) bright field image revealing Widman-
          statten precipitate pattern, high dislocation density, and
          twinning at "C"; b) dark field image of spots A in (C),
          showing only precipitate contrast is reversed; c) selected
          area diffraction; extra reflections are due only to Fe_3C.

Fig. 5   Thin foil micrographs of Fe/Mo/C steel, tempered 30 minutes
          at 375°C. Orientation [311], a) bright field image showing
          Fe_3C precipitates and dislocation entanglements; b) dark
          field image of (a) using an Fe_3C reflection. Compare to
          Fig. 4.

Fig. 6   Fe/Cr/C steel DSA at 600°C; dark field image showing recrystalli-
          zed structure with spherodized precipitates (B) and recovered
          dislocations (A); orientation [311].

Fig. 7   Fe/Mo/C steel tempered 30 minutes at 600°C a) dark field image
          obtained from region A in (c); b) bright field image -- notice
          fine plates in one orientation (compare to Figs. 4-6) and some
          spherodized cementite (B); c) selected area diffraction showing
          streaks due to fine plates; cementite spots at C; foil in [311].

Fig. 8   Thin foil micrographs of Fe/Cr/C steel, DSA at 125°C

a) bright field image showing dislocation contrast and strain

fields around precipitates; b) dark field image of (a) showing

reversal of contrast of precipitates. Orientation [311].

Fig. 9   Thin foil micrographs of Fe/Cr/C steel after DSA at 375°C;

[111] foil. a) bright field image revealing dislocation tangles

around distorted precipitates. Notice fine background of

precipitates on dislocations e.g. near B, C; dislocations tilted

out of strong contrast so that particles are more easily

visible.

REFERENCES

1. G. Thomas, V. F. Zackay, and E. R. Parker, "Structure and High Strength Metals", Strengthening Mechanisms, J. J. Burke, N. L. Reed and V. Weiss, Syracuse University Press, Syracuse, N. Y., (1966) 3.

2. G. R. Speich and H. Warlimont, "Yield Strength and Transformation Substructure of Low Carbon Martensite", J. Iron Steel Inst. 206 (1968) 385.

3. E. B. Kula, "Strengthening of Steels by Thermomechanical Treatments", Strengthening Mechanisms, J. J. Burke, N. L. Reed and V. Weiss, Syracuse University Press, Syracuse, N. Y., (1966) 83.

4. E. T. Stephenson, and M. Cohen, "The Effect of Prestraining and Retempering on AlS1 Type 4340", Trans. ASM 54, (1961) 72.

5. A.S. Keh and W. C. Leslie, "Recent Observations on Quench Aging and Strain Aging of Iron and Steel", Materials Science Research, H. H. Stadelmier, John Wiley and Sons, Inc., New York, N. Y., (1963) 208.

6. D. J. Schmatz, "Thermomechanical Treatments", Met. Eng. Quart. ASM 6 (1966) 20.

7. G. Thomas, D. Schmatz, and W. Gerberich, "Structure and Strength of Some Ausformed Steels, High Strength Materials, V. F. Zackay, John Wiley and Sons, Inc., New York, N. Y. (1965) 251.

8. V. F. Zackay, W. W. Gerberich, R. Busch, and E. R. Parker, "The Strength and Toughness of Dynamically Strain Aged Alloy Steel Sheets", Intern. J. of Fracture Mechanics, 2 No. 4, (1966) 638.

9. B. J. Brindley and J. T. Barney, "Dynamic Strain Aging in Mild Steel', Acta Met 14, (1966) 1765.

10. A. S. Keh and H. A. Wriedt, "An Electron Transmission Study of Nitride Precipitation in Alpha Iron", Trans. AIME 224, (1962) 560.

11. D. V. Wilson and B. Russell, "The Contribution of Precipitation to Strain Aging in Low Carbon Steels," Acta Met 8, (1960) 468.

12. E. Bain and H. W. Paxton, Alloying Elements in Steels, 2nd ed. ASM, Metals Park, Ohio (1961) 148.

13. R. W. K. Honeycombe, H.J. Harding, and J. J. Irani, "Strengthening Mechanisms in Ferritic and Austenitic Steels", High Strength Materials, V. F. Zackay, John Wiley and Sons, Inc., New York, N. y., (1965) 213.

14. W. Pitsch and A. Schrader, "Die Ausschiedungsform des Zementits in Ferrit", Arch. Eisen. 29, (1958) 485.

15. A. J. Baker, P. M. Kelly, and J. Nutting, "Structures Resulting from Phase Transformations in Steels", Electron Microscopy and Strength of Crystals, G. Thomas and J. Washburn, Interscience Publishers, New York, N. Y., (1963) 899.

16. G. V. Kurdjumov, "Phenomena Occurring in the Quenching and Tempering of Steels', J. Iron Steel Inst. 195, (1960) 26.

17. P. M. Kelly and J. Nutting, "The Martensite Transformation in Carbon Steels", Proc. Roy. Soc 259, (1960) 45.

18. P. M. Kelly and J. Nutting, "The Morphology of Martensite", J. Iron Steel Inst. 197, (1961) 199.

19. P. J. Fopiano, S. Das Gupta and D. Kalish, ManLabs, Inc., Tech. Rept. 320.4/4-3, June (1962).

20. K. Tekin and P. M. Kelly, "A Study of the Tempering of Steel Using Transmission Electron Microscopy", Precipitation from Iron-Base Alloys, G. R. Speich and J. B. Clark, Gordon and Breach Science Publishers, New York, N. Y., (1965) 173.

21. D. Raynor, J. A. Whiteman, and R. W. K. Honeycombe, "Precipitation
     of Molybdenum and Vanaduim Carbides in High Purity Iron Alloys",
     J. Iron Steel Inst., 204, (1966) 349.

22. K. Kuo, "Carbides in Chromium, Molybdenum and Tungsten Steels", J. Iron
     Steel Inst., 173, (1965) 363.

23. J. H. Woodhead and A. G. Quarrell, "Role of Carbides in Low Alloy
     Creep Resisting Steels', J. Iron Steel Inst. 203, (1965) 605.

24. J. Beech and D. H. Warrington, "M_7C_3 to $M_{23}C_6$ Transformation in Chromium
     Containing Alloys", J. Iron Steel Inst., 204, (1966) 460.

25. W. C. Leslie and A. S. Keh, "An Electron Transmission Study of the
     Strain Aging of Iron", J. Iron Steel Inst. 200, (1962) 722.
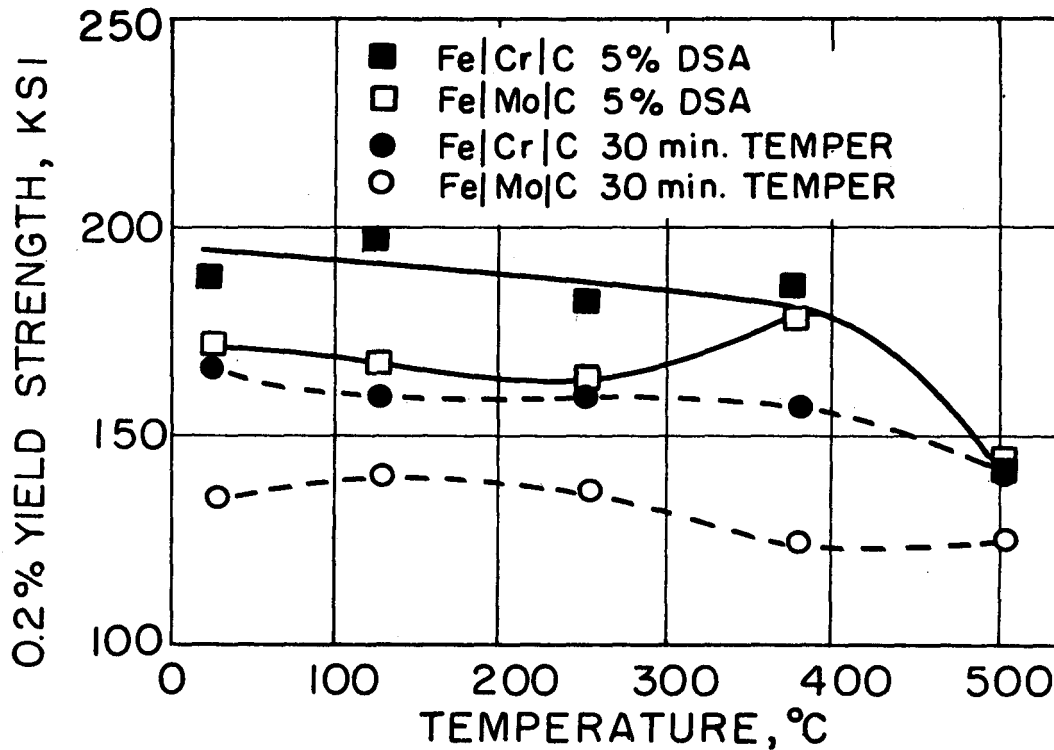
XBL 688-5652

Fig. 1
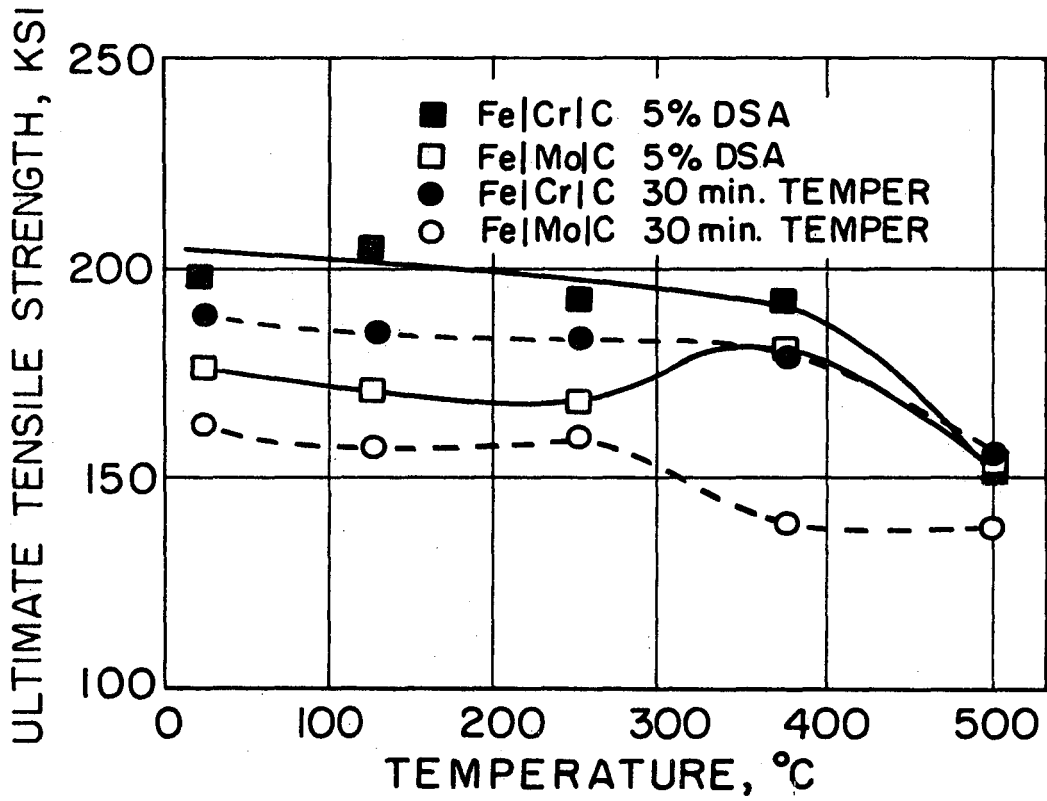
Fig. 2
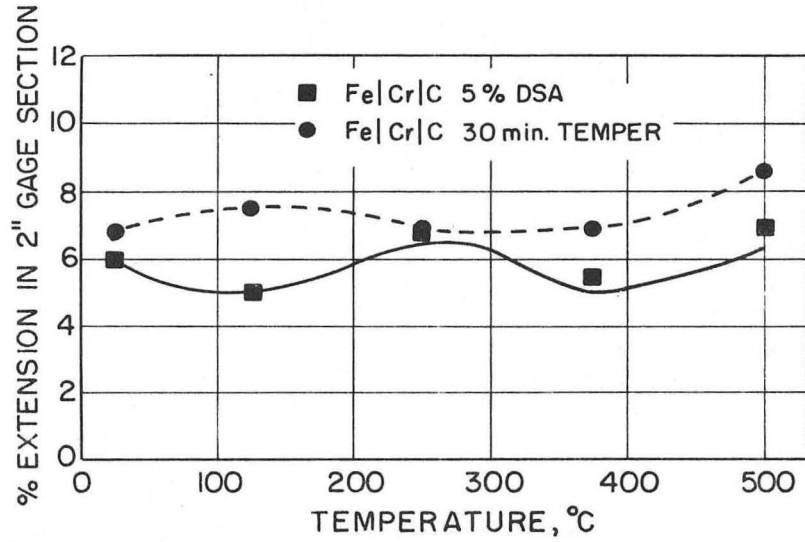
XBL 688-5653

(a)
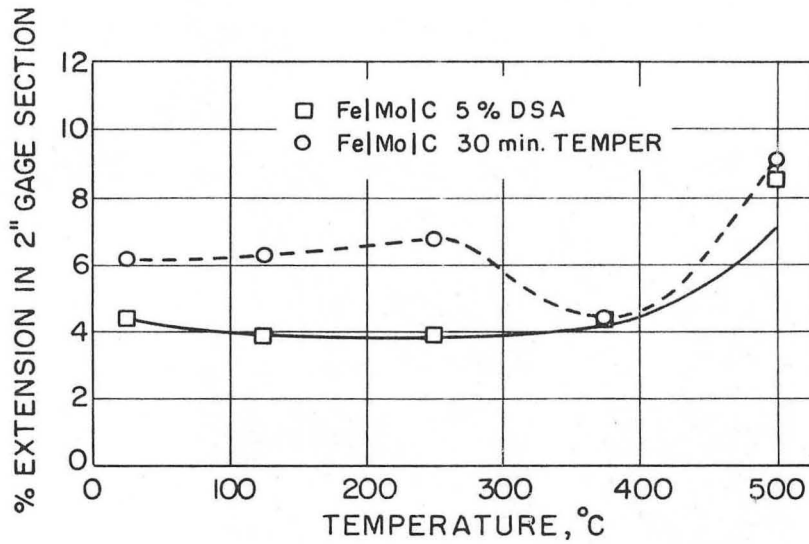
(b)

XBL 688-5654

Fig. 3
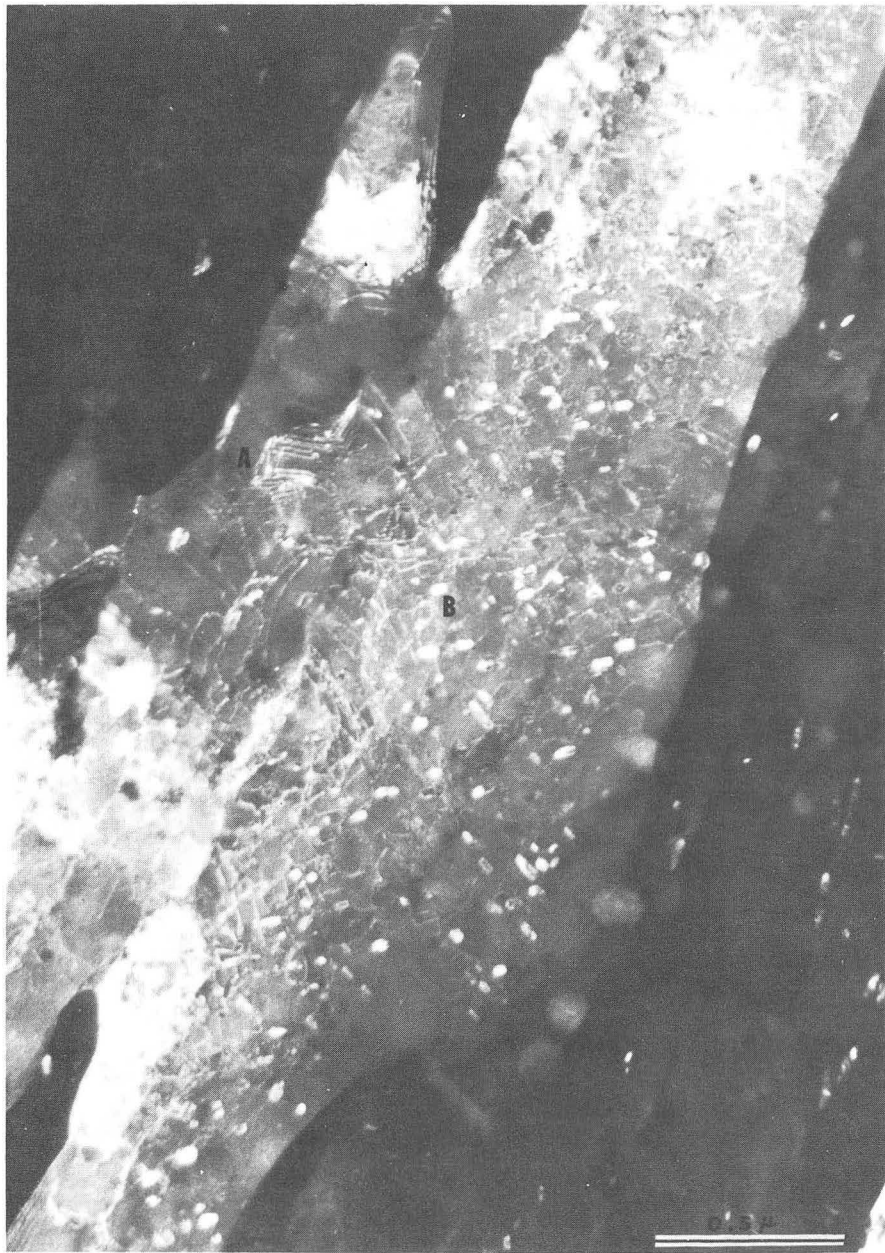
XBB 685-3028

Figure 6
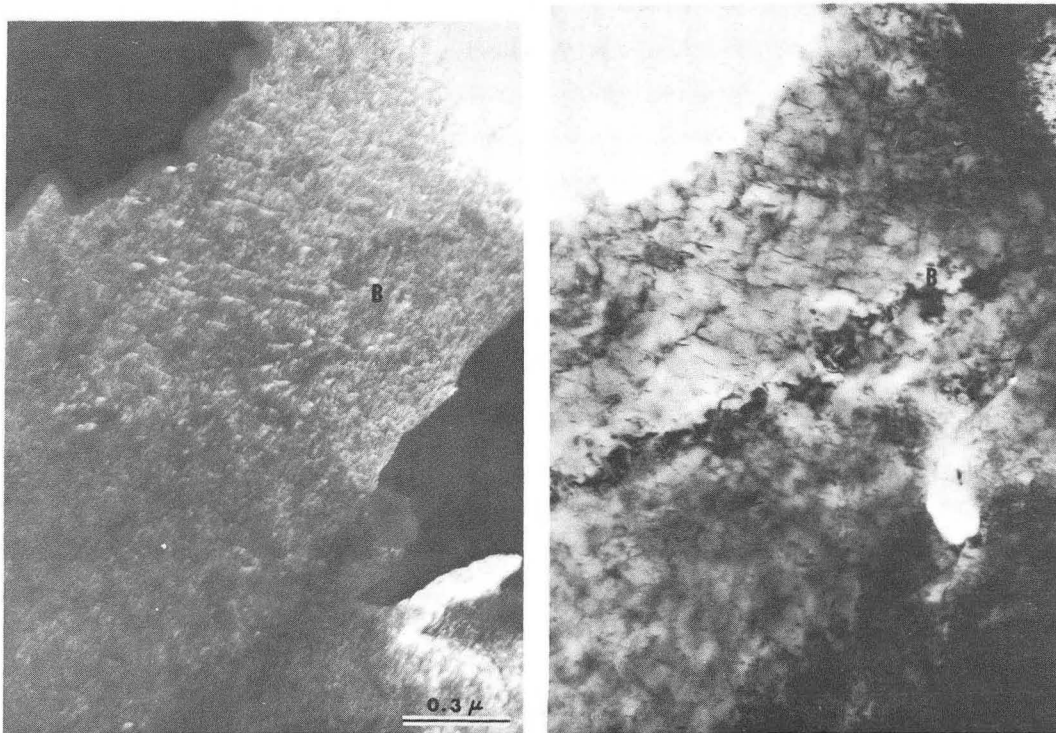
(a)

(b)
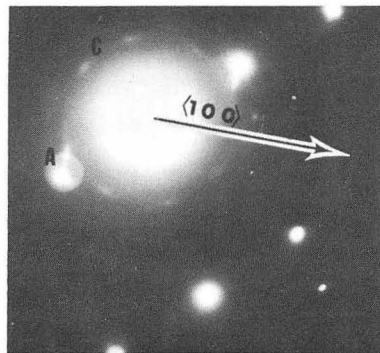
(c)

XBB 685-3108

Figure 7

(a)

(b)   XBB 685-3011

Figure 8

(a)

(c)

(b)

XBB 685-3026

Figure 9